Front. Mater. Sci. 2014, 8(4): 354–362
DOI 10.1007/s11706-014-0270-8

RESEARCH ARTICLE

Fabrication and characterization of curcumin-loaded silk fibroin/P(LLA-CL) nanofibrous scaffold

Yuan LIAN[1], Jian-Chao ZHAN[1], Kui-Hua ZHANG (✉)[1], and Xiu-Mei MO[2]

1 College of Materials and Textile Engineering, Jiaxing University, Jiaxing 314001, China
2 Biomaterials and Tissue Engineering Laboratory, College of Chemistry and Chemical Engineering and Biological Engineering, Donghua University, Shanghai 201620, China

ABSTRACT: Curcumin exhibited excellent properties including antioxidant, anti-inflammatory, antiviral, antibacterial, antifungal, anticancer, and anticoagulant activities. In this study, curcumin was incorporated into silk fibroin (SF)/poly(L-lactic acid-*co*-e-caprolactone) (P(LLA-CL)) nanofibrous scaffolds via electrospinning, and changes brought about by raising the curcumin content were observed: SEM images showed that the average nanofibrous diameter decreased at the beginning and then increased, and the nanofibers became uniform; FTIR showed that the conformation of SF transforming from random coil form to β-sheet structure had not been induced, while SF conformation converted to β-sheet after being treated with 75% ethanol vapor; XRD results confirmed that the crystal structure of (P(LLA-CL)) had been destroyed; The mechanical test illustrated that nanofibrous scaffolds still maintained good mechanical properties. Further, curcumin-loaded nanofibrous scaffolds were evaluated for drug release, antioxidant and antimicrobial activities *in vitro*. The results showed that curcumin presented a sustained release behavior from nanofibrous scaffolds and maintained its free radical scavenging ability, and such scaffolds could effectively inhibit *S. aureus* growth (> 95%). Thus, curcumin-loaded SF/P(LLA-CL) nanofibrous scaffolds might be potential candidates for wound dressing and tissue engineering scaffolds.

KEYWORDS: curcumin; SF/P(LLA-CL); nanofibrous scaffold; control release

Contents

Received August 29, 2014; accepted October 24, 2014

E-mail: zhangkuihua@126.com

1 Introduction

Curcumin, derived from the rhizome of perennial herb Curcuma longa, is a low molecular weight natural yellow-orange polyphenol compound [1]. Extensive studies had exhibited that it possessed good antioxidant, anti-inflammatory, antiviral, antibacterial, antifungal, anticancer, anticoagulant activities, and so on [2–3]. However, curcumin presented extremely low solubility in aqueous solutions, instability in alkaline conditions, thermal treatment and light and easy aggregation when administered intravenously [4]. These disadvantages usually limited its applications in medicine fields. In order to enhance its therapeutic effects, curcumin was incorporated in microgels, hydrogel, porous sponge scaffold, nanofibers and so on [5–8].

Silk fibroin (SF) is an attractive natural fibrous protein for biomedical applications due to its unique properties, including good biocompatibility, biodegradability, desirable oxygen and water permeability, lower inflammatory and commercial availability at relatively lower cost [9–10]. However, SF nanofibrous scaffolds presented poor mechanical properties. In previous studies, we successfully fabricated SF/poly(L-lactic acid-*co*-e-caprolactone) (SF/P(LLA-CL)) nanofibrous scaffolds with good biocompatibility both *in vitro* and *in vivo* in order to improve mechanical properties of nanofibrous scaffolds [11–12]. Moreover, aligned SF/P(LLA-CL) nanofibrous nerve guidance conduits could promoted peripheral nerve regeneration [13–14]. However, it was easy to cause inflammation of the organization and bacterial infections at the beginning of the scaffolds implanted in the body. So, it was imperative that the releasing small molecules from scaffolds resisted or alleviated symptoms. To endow with anti-inflammatory, antioxidant, antibacterial, activities of SF/P(LLA-CL) nanofibrous scaffolds for further application in tissue regeneration or wound dress, in the present study, curcumin-loaded SF/P(LLA-CL) nanofibrous scaffolds were fabricated and characterized. Sustained release of curcumin from nanofibrous scaffolds and antibacterial and antioxidant properties of nanofibrous scaffolds were investigated.

2 Experimental

2.1 Materials

Cocoons of *Bombyx mori* silkworm were kindly supplied by Jiaxing Silk Co. Ltd. (China). A copolymer of P(LLA-CL) (50:50), which has a composition of 50 mol.% L-lactide, was used provided by Nara Medical University (Japan). 1,1,1,3,3,3-Hexafluoro-2-propanol (HFIP) was purchased from Daikin Industries Ltd. (Japan). Ethanol was obtained from Chemical Reagent Co., Ltd. (China). Curcumin was purchased from Shanghai Winverb Medical Technology Co., Ltd.

2.2 Preparation of regenerated SF

Raw silk was degummed three times with 0.5 wt.% Na_2CO_3 solution at 100°C for 30 min each and then washed with distilled water. Degummed silk was dissolved in a ternary solvent system of $CaCl_2/H_2O$/ethanol solution (mole ratio: 1/8/2) for 1 h at 70°C. After dialysis through cellulose tubular membrane (250-7u, Sigma) in distilled water for 3 d at room temperature, the SF solution was filtered and lyophilized to obtain regenerated SF sponges.

2.3 Preparation of curcumin-loaded SF/P(LLA-CL) nanofibrous scaffolds

Curcumin is dissolved in HFIP with different concentrations at ultrasonic treatment and then the regenerated SF sponges and P(LLA-CL) dissolved into curcumin HFIP solution to render SF/P(LLA-CL) (the mass ratio of SF and P(LLA-CL) was 1:1) at the concentration of 8.0% (w/v). The contents of curcumin were 2.0%, 4.0% and 6.0% (w/w) based on the weights of SF and P(LLA-CL), respectively. The blended solution was loaded into a 2.5 mL plastic syringe with a blunt-ended needle with an inner diameter of 0.21 mm. The needle is located 150 mm above a grounded solid collector. A syringe pump (789100C, Cole-Parmer, America) was used to feed solutions to the needle tip at a feed rate of 1.2 mL/h. A high voltage of 10 kV was generated between the needle and ground collector using a high-voltage power supply (BGG6-358, BMEICO, China). To improve water-resistant ability, the collected nanofibrous scaffolds were treated with 75% (v/v) ethanol

vapor for 24 h as described before [12], and then dried under vacuum for 1 week at room temperature.

2.4 Characterization of nanofibrous scaffolds

The morphology and diameter of electrospun fibers were observed with scanning electron microscopy (SEM; JSM-5600) at an acceleration voltage of 10 kV. The diameter range of the nanofibers was measured basing on SEM images using the image visualization software Image-J 1.34 s (National Institutes of Health) and calculated by selecting 100 fibers randomly observed on the SEM images.

Fourier transform infrared spectra (FTIR) were obtained on AVATAR 380 FTIR instrument (Thermo Electron, Waltham, MA). All spectra were recorded by an absorption mode in the wave length range of 4000–500 cm^{-1}.

Wide-angle X-ray diffraction (WAXD) curves were obtained on an X-ray diffractometer (Rigaku, Japan) within the scanning region of 2θ (5°–50°), with Cu Kα radiation (λ = 1.5418 Å) at 40 kV and 40 mA.

2.5 Mechanical property measurements

Mechanical properties were obtained by applying tensile test loads to specimens prepared from the electrospun scaffolds with different curcumin content according to the method reported in the literature [13]. Mechanical properties were tested by a materials testing machine (H5K-S, Hounsfield, England) at the temperature of 20°C and a relative humidity of 65% and an elongation speed of 10 mm/min. Each sample was measured six times. The specimen thicknesses were measured using a digital micrometer, having a precision of 1 μm.

2.6 Release studies *in vitro*

A certain amount nanofibrous scaffolds were dissolved in HFIP at 37°C for 6 h. The solution was filtrated through a 0.22 μm filter (RF-jet) and then measured at 422 nm using an ultraviolet (UV) spectrophotometer (UV-2102pcs, UNICO (Shanghai) Instruments Co., Ltd.). The actual amount of curcumin in nanofibrous scaffolds was determined from the obtained data against a predetermined calibration curve for curcumin. The percentage of encapsulation efficiency (φ_{ee}) was then calculated as follows:

$$\varphi_{ee}/\% = \frac{c_a/g}{c_i/g} \times 100 \quad (1)$$

where c_a was the calculated amount of the encapsulated curcumin and c_i was the initial amount of curcumin used for electrospinning. The release of curcumin from SF/P (LLA-CL) nanofibrous scaffolds was carried out over a period of 72 h. Samples were incubated in phosphate buffered saline (PBS) containing 2.5% (w/v) tween 80 with a continuous swing of 90 r/min at 37°C. At a specified period between 0 and 72 h, 3 mL of the release solution was withdrawn and an equal volume of PBS containing 2.5% (w/v) tween 80 was refilled. The amount of curcumin in the sample is determined using UV detector (422 nm). Each value was averaged from three specimens.

2.7 Antioxidant activity *in vitro*

The antioxidant activity of curcumin-loaded nanofibrous scaffolds was assessed with 1,1-diphenyl-2-picrylhydrazyl (DPPH) free radical scavenging assay [15]. A certain amount of curcumin-loaded SF/P(LLA-CL) nanofibrous scaffolds was first dissolved in 2 mL of HFIP and then added 1 mL ethanol solution of 100 mmol/L DPPH. The samples were incubated in dark for 30 min, and the absorbance was measured in a spectrophotometer at 517 nm. The percentage of antioxidant activity η_{aa} (the radical scavenging activity) was calculated according to the following equation:

$$\eta_{aa}/\% = \frac{A_{control} - A_{sample}}{A_{control}} \times 100 \quad (2)$$

where $A_{control}$ and A_{sample} are the absorbance values of the solution with and without the samples, respectively. Each value was averaged from three specimens.

2.8 Antibacterial activity *in vitro*

The antibacterial activity of curcumin-loaded nanofibrous scaffolds was tested using evaluated by the turbidity measurement method against *Staphylococcus aureus* (*S. aureus*; G+) [16]. *S. aureus* were reconstituted in nutrient broth. The bacteria solution was standardized to an absorbance value between 0.1 and 0.2 at 625 nm (equivalent to 0.5 McFarland standard) and aliquot into 10 mL volumes. A certain amount of curcumin-loaded nanofibrous scaffolds were added. All tested solutions were incubated at 37°C with constant shaking, and the absorbance at 625 nm was monitored after 24 h of incubation. The percentage of bacterial inhibition (σ_{bi}) was calculated by the absorbance difference between the bacteria solutions with and without samples after 24 h using the following equation:

$$\sigma_{bi}/\% = \frac{I_{control} - I_{sample}}{I_{control}} \times 100 \quad (3)$$

where $I_{control}$ and I_{sample} are the absorbance of the control bacteria solution without scaffolds and of the bacteria solution with the sample, respectively, at 625 nm after 24 h. Each value was averaged from three specimens

3 Results and discussion

3.1 Morphology of curcumin-loaded SF/P(LLA-CL) nanofibers

SEM images and diameter distributions of SF/P(LLA-CL) nanofibrous scaffolds with different curcumin contents were observed in Fig. 1. The average diameter of nanofibers gradually decreased from (461±215) to (293±110) nm with the increase of the curcumin content from 0.0% to 4.0% (w/w). However, the average diameter of nanofibers increased to (497±118) nm and the nanofibers became uniform when the curcumin content increased to 6.0% (w/w). The reasons may be as follows: the increase of solution conductivity resulted in larger elongation forces for the fibre jet to yield smaller fibres with the addition of the low molecular weight curcumin at the beginning [17]. On the other hand, the curcumin molecule possessed hydroxyl (–OH) and carbonyl (–C = O), and SF had hydroxyl (–OH), amino ($–NH_2$) and carboxyl (–COOH). The strong intermolecular hydrogen bonds interaction between SF and curcumin lead to the increase of solution viscosity. Moreover, the crystal structure was destroyed to give rise to the increase of solution viscosity (seen from Fig. 3).

3.2 FTIR analysis

FTIR results of curcumin, electrospinning SF/P(LLA-CL), curcumin-loaded SF/P(LLA-CL) nanofibers before and after being treated with 75% (v/v) ethanol vapor were shown in Figs. 2(a) and 2(b). The FTIR of curcumin showed the absorption band at 3431 cm^{-1} which was attributed to the phenolic (–OH) stretching vibration, and at 2924 and 2849 cm^{-1} which were attributed to $–CH_3$ and $–CH_2$ stretching vibrations, respectively. The bands at 1633, 1599, 1511, 1450, 1275, 1139 cm^{-1} were attributed to C = C stretching vibrations, stretching vibrations of the benzene ring, aromatic C–O stretching and C–O–C stretching vibration [18]. The FTIR of electrospun SF/P(LLA-CL) showed the absorption band at 3295 cm^{-1}, which was attributed to the stretching vibrations of $–NH_2$ and –OH of SF. The absorption bands at 2940 and 2862 cm^{-1} were attributed to the stretching vibration of $–CH_3$ or $–CH_2$ of P(LLA-CL). The characteristic absorption bands at 1756 and 1735 cm^{-1} were attributed to ester bonds (–COO) of PLLA chain segments and PCL chain segments, respectively in P(LLA-CL). The absorption bands at 1652 (amide I), 1540 (amide II) and 1240 cm^{-1} (amide III) were assigned to the SF with random coil conformation [19]. The curcumin-loaded SF/P(LLA-CL) nanofibers showed absorption bands at 1648 (amide I), 1538 (amide II) and 1240 cm^{-1} (amide III). These absorption bands showed no obvious difference in comparison with SF/P(LLA-CL). The conformation of SF still existed in random coil or α-helix. The result clarified that curcumin did not induce SF conformation from random coil or α-helix to β-sheet. After being treated with 75% (v/v) ethanol vapor, the absorption bands at 1648 (amide I) and 1533 (amide II) shifted to 1630 and 1520 cm^{-1}, respectively, which were attributed to the SF with β-sheet conformation (silk II). Therefore, 75% (v/v) ethanol vapor could transform the crystal structure of SF from random coil or α-helix (soluble in water) to β-sheet (insoluble in water).

3.3 X-ray diffraction analysis

X-ray diffraction (XRD) patterns of curcumin, electrospun SF/P(LLA-CL), curcumin-loaded SF/P(LLA-CL) nanofibers before and after being treated with 75% (v/v) ethanol vapor were shown in Figs. 3(a) and 3(b). Pure curcumin existed in a crystalline state, displaying a number of characteristic reflection peaks at 2θ between 10° and 30°. The electrospinning SF/P(LLA-CL) fibrous scaffolds showed peaks at 2θ (16.7°, 18.9° and 22.4°), respectively. The peak at 2θ 16.7° was attributed to the crystalline diffraction peak of PLLA chain segment, and peaks at 2θ 18.9° and 22.4° were attributed to the crystalline diffraction peak of PCL chain segments [20]. The curcumin-loaded SF/P(LLA-CL) fibrous scaffolds showed that the peak at 2θ 16.7° disappeared. The results indicated that the crystalline structure of PLLA chain segments was damaged with the addition of curcumin. The curcumin-loaded SF/P(LLA-CL) fibrous scaffolds after being treated with 75% (v/v) ethanol vapor showed peaks at 2θ = 11.8°, 19.9°, 24.3°. These peaks resemble those of structure (silk II) [21]. Moreover, the peak intensity at 2θ = 16.7° increased after being treated with 75% (v/v) ethanol vapor. The results clarified that 75% (v/v) ethanol vapor maybe induce the crystalline of PLLA chain segments in P(LLA-CL).

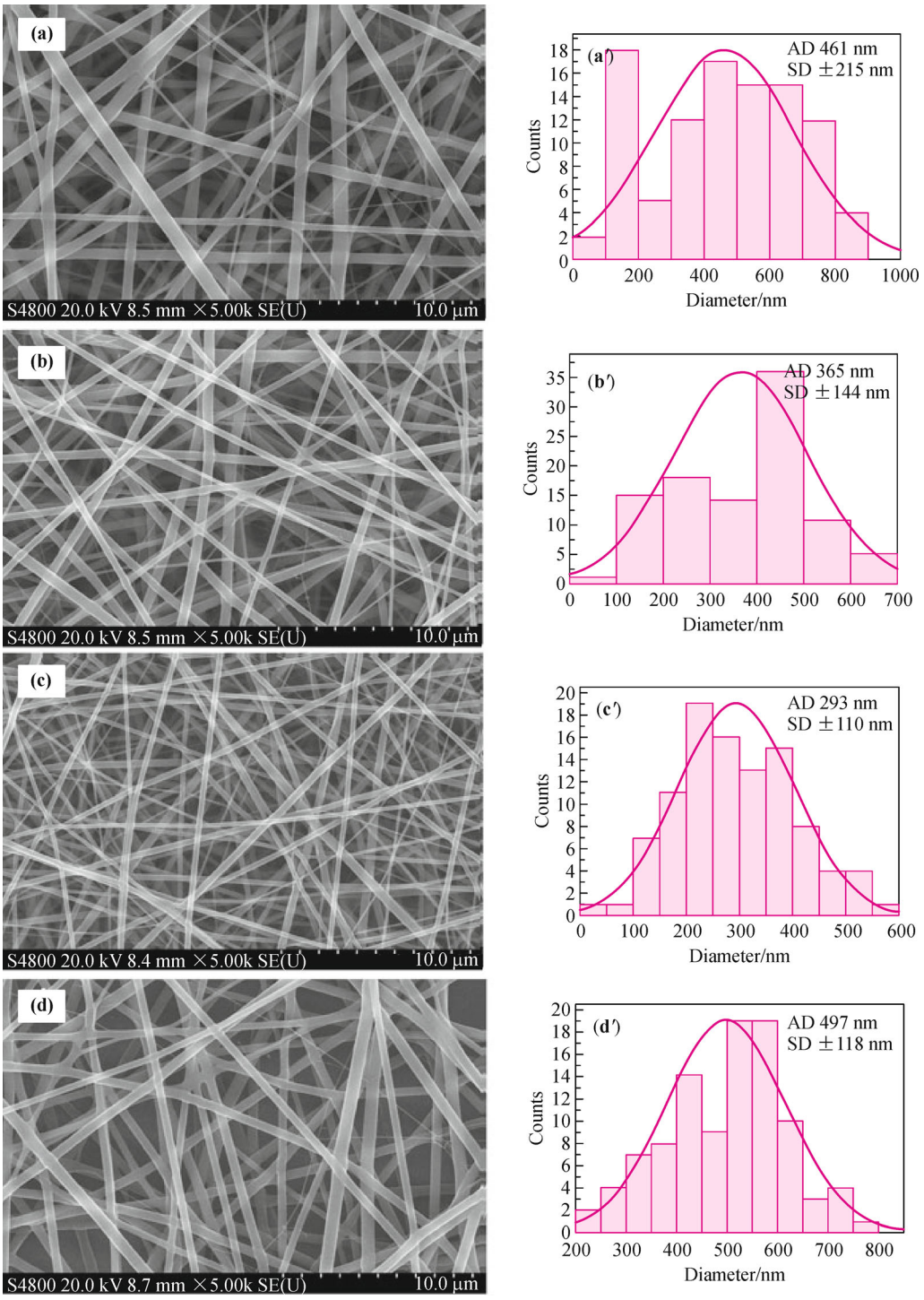

Fig. 1 SEM images and diameter distributions of nanofibers with different curcumin content: **(a)(a′)** 0.0; **(b)(b′)** 2.0% (w/w); **(c)(c′)** 4.0% (w/w); **(d)(d′)** 6.0% (w/w).

3.4 Mechanical property analysis

The typical tensile stress–strain curves of SF/P(LLA-CL) nanofibrous scaffolds with different curcumin content were shown in Fig. 4. The average elongation at break and average tensile strength of each specimen were summarized in Table 1. As the curcumin content was 2.0% and 4.0% (w/w), respectively, the stress and the strain had no obvious changes in comparison with SF/P(LLA-CL) nanofibrous scaffolds. However, when the curcumin

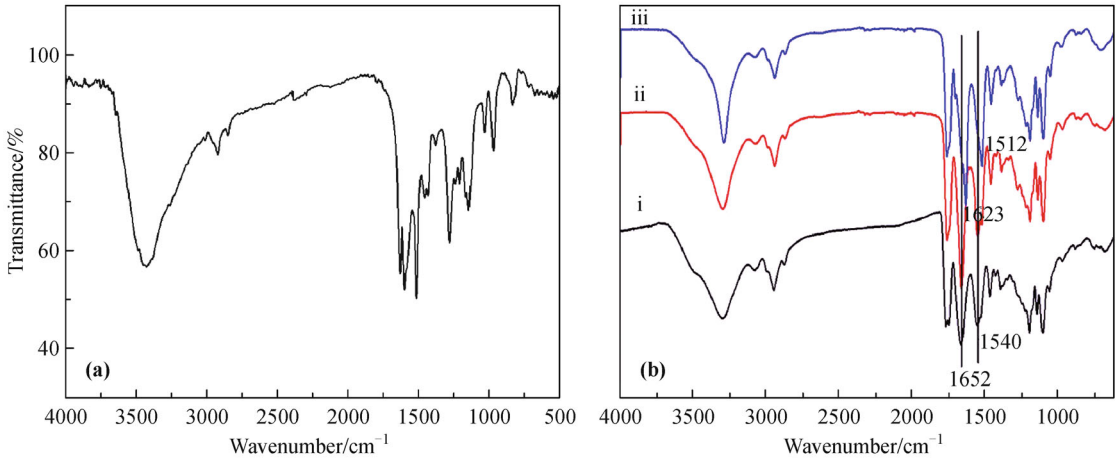

Fig. 2 FTIR results of **(a)** curcumin and **(b)** SF/P(LLA-CL) nanofibrous scaffolds: SF/P(LLA-CL) nanofibers (i); curcumin-loaded SF/P (LLA-CL) nanofibers (ii); curcumin-loaded SF/P(LLA-CL) nanofibers after being treated with 75% (v/v) ethanol vapor (iii).

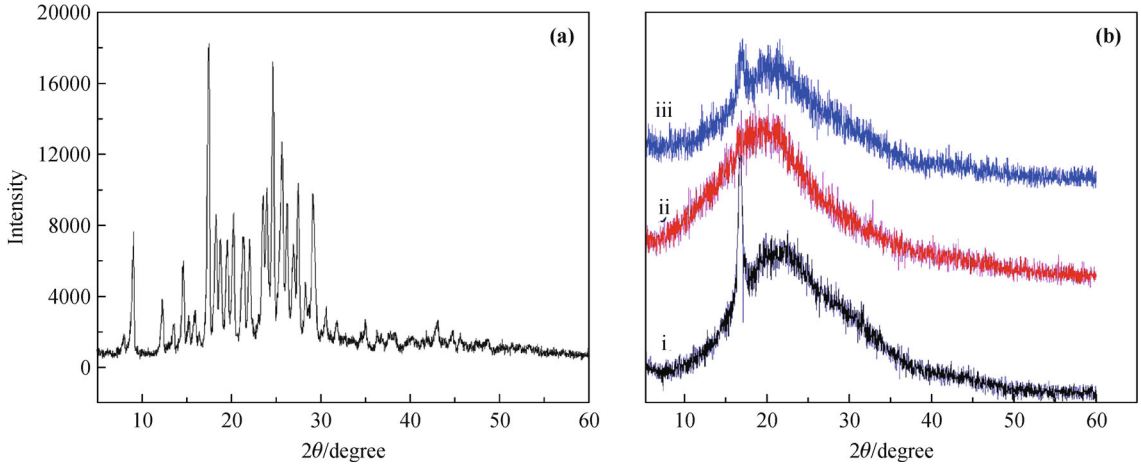

Fig. 3 XRD patterns of **(a)** curcumin and **(b)** SF/P(LLA-CL) nanofibrous scaffolds: SF/P(LLA-CL) nanofibers (i); curcumin-loaded SF/P(LLA-CL) nanofibers (ii); curcumin-loaded SF/P(LLA-CL) nanofibers after being treated with 75% (v/v) ethanol vapor (iii).

content increased to 6.0% (w/w), the average elongation at break had a palpable increase (117.44±1.35)%, and the average tensile strength had a slightly increase (5.27±0.34) MPa. This was possibly because the nanofibers with 6.0% (w/w) curcumin content became more uniform and thicker than other nanofibers (seen from Fig. 1), which helped the scaffolds to withstand higher stress.

3.5 Release of curcumin from nanofibrous scaffolds *in vitro*

The actual amount of curcumin in nanofibrous scaffolds was determined through a certain amount of curcumin-loaded SF/P(LLA-CL) nanofibrous scaffold without treatment with 75% (v/v) ethanol vapor being dissolved in HFIP. The encapsulation efficiency values of scaffolds with the curcumin contents of 2.0%, 4.0% and 6.0% (w/w) were 70.23%, 73.36% and 75.21%, respectively. The cumulative release amount of curcumin was reported as the percentage of the actual amount of curcumin present in the sample. The release curves of curcumin from nanofibers were shown in Fig. 5. The release curves had no significant difference among with three curcumin-loaded nanofibrous scaffolds. They exhibited a slightly burst release of curcumin during the beginning 12 h, then reach a sustain release over 72 h. Generally, the increase of drug content lead to a larger concentration gradient, and hence a higher diffusion driving force promoted drug release [18]. However, the curcumin presented similar accumulative release amount when the curcumin content was 4.0% and 6.0% (w/w) in nanofibrous scaffolds, respectively. This may cause that the diameter of nanofibers containing 4.0%

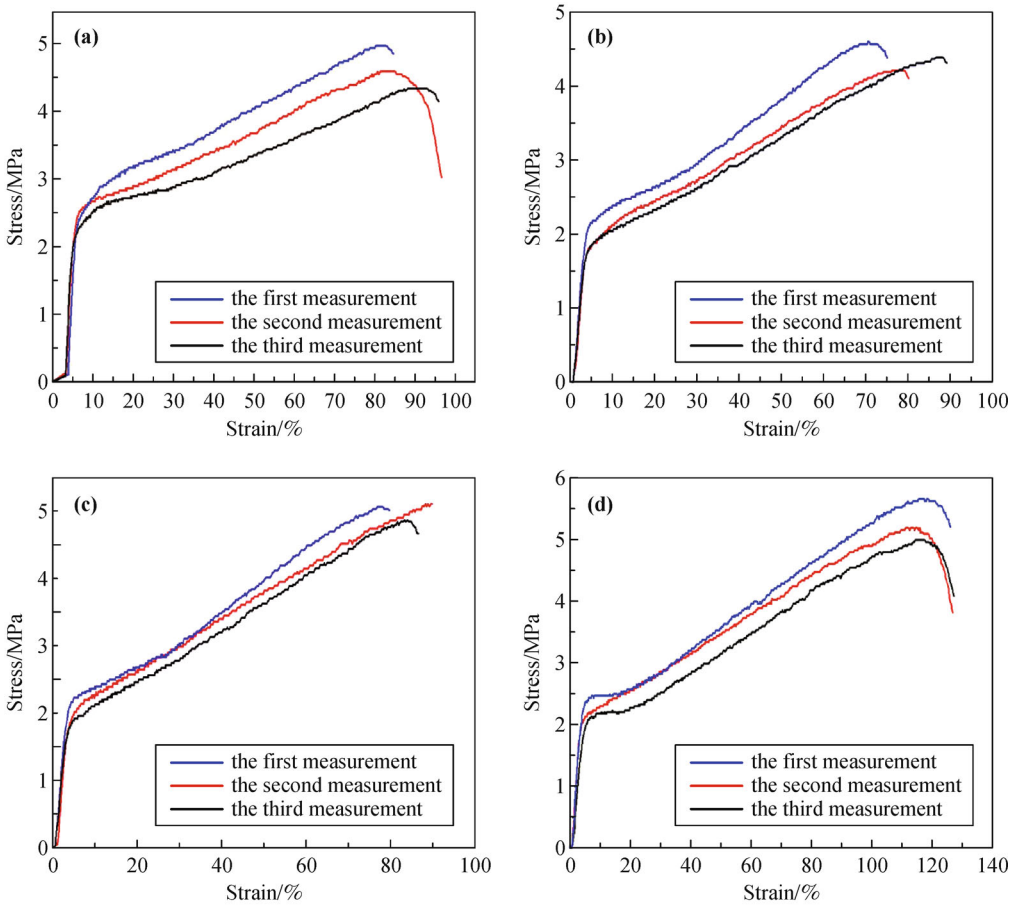

Fig. 4 Mechanical properties of SF/P(LLA-CL) nanofibrous scaffolds with different curcumin contents: **(a)** 0.0; **(b)** 2.0% (w/w); **(c)** 4.0% (w/w); **(d)** 6.0% (w/w).

Table 1 Mechanical properties of SF/P(LLA-CL) nanofibrous scaffolds with various curcumin contents

Curcumin content /(%, w/w)	Specimen thickness /mm	Elongation at break /%	Tensile strength /MPa
0	0.138±0.021	87.02±5.34	4.64±0.32
2.0	0.118±0.010	79.91±7.78	4.38±0.17
4.0	0.099±0.017	83.86±5.87	5.00±0.13
6.0	0.102±0.012	117.44±1.35	5.27±0.34

(w/w) curcumin is thinner than those of 6.0% (w/w), resulting in quicker release of curcumin from nanofibers. According to previous results, SF/P(LLA-CL) nanofibrous scaffolds were not degradable in a short time [22]. So the curcumin release from SF/P(LLA-CL) nanofibrous scaffolds mainly resulted from diffusion release behavior of curcumin from SF/P(LLA-CL) nanofibrous scaffolds.

3.6 Antioxidant activity *in vitro*

The antioxidant activity of SF/P(LLA-CL) nanofibrous scaffolds with different curcumin content was estimated by using a DPPH-free radical scavenging assay and the results were shown in Fig. 6. The radical scavenging activity of SF/P(LLA-CL) nanofiber scaffolds was 32.2%. The results clarified that SF/P(LLA-CL) nanofibers helped in retaining free radical scavenging property. This could be attributed to tyrosine in the SF possessing antioxidant function [23]. Compared with that of SF/P(LLA-CL) nanofiber scaffolds, the curcumin-loaded SF/P(LLA-CL) nanofiber scaffolds had significant scavenging influence on the DPPH radical and the influence gradually increased with the increase of curcumin content in the range of 2.0%–6.0% (w/w). The results demonstrated that curcumin-loaded nanofibrous scaffolds possessed good antioxidant activity. Previous studies reported that curcumin could inhabit peroxidation

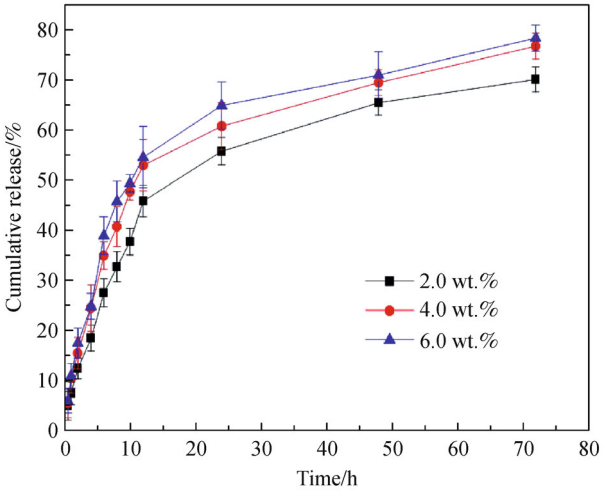

Fig. 5 Release curves of curcumin from SF/P(LLA-CL) nanofibrous scaffolds *in vitro*.

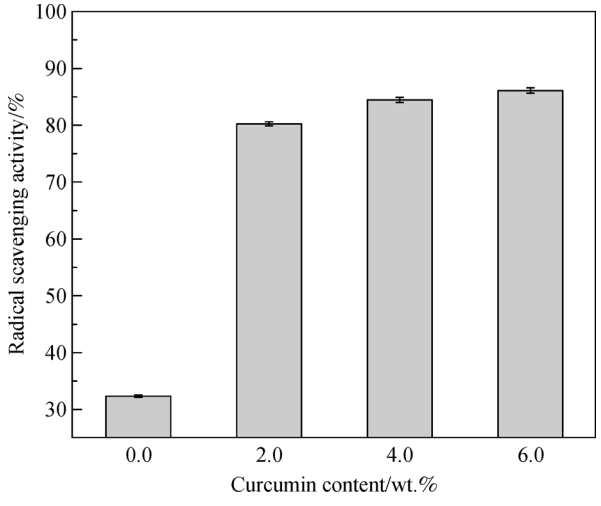

Fig. 6 Radical scavenging activity of SF/P(LLA-CL) nanofibrous scaffolds with different curcumin content (n = 3).

of human low density lipoprotein (LDL), oxidation of protein and the activity of inducible nitric oxide synthase (iNOS) [24]. Therefore, the incorporation of curcumin in nanofibrous scaffolds was beneficial to improving antioxidant properties of scaffolds for biomedical application.

3.7 Antibacterial activity *in vitro*

The antibacterial activity of curcumin-loaded SF/P(LLA-CL) nanofibrous scaffolds was tested to examine their ability to inhibit bacterial growth in a dynamic system (scaffolds mixed with *S. aureus* bacterial liquid cultures) and shown in Table 2. SF/P(LLA-CL) nanofiber scaffolds without curcumin showed 15.8% inhibition of bacterial growth, while those with the curcumin content from 2.0% to 6.0% (w/w) showed a remarkable increase of the inhibition of bacterial growth approaching to 100%. This was caused by that the sustained releasing curcumin from SF/P(LLA-CL) nanofibrous scaffolds in bacterial liquid cultures inhibited bacterial growth. The results indicated that curcumin-loaded SF/P(LLA-CL) nanofiber scaffolds exhibited good antibacterial activity.

Table 2 Bacterial inhibition percentage of SF/P(LLA-CL) nanofiber scaffolds with different curcumin content (n = 3)

Content of curcumin /(%, w/w)	Bacterial inhibition /%
0.0	15.8±0.53
2.0	98.3±0.29
4.0	99.3±0.13
6.0	99.7±0.85

4 Conclusions

In the present study, curcumin-loaded SF/P(LLA-CL) nanofibrous scaffolds were successfully fabricated. Curcumin exhibited a sustained release from nanofibrous scaffolds. The addition of curcumin into scaffolds prominently strengthened antioxidant and antibacterial activities of nanofibrous scaffolds. Our ongoing studies will focus on the interaction between nanofibrous scaffolds and cells *in vitro*, and then the histocompatibility *in vivo* for further application of curcumin-loaded SF/P(LLA-CL) nanofibrous scaffolds in tissue engineering and would dressing.

Abbreviations

DPPH	1,1-diphenyl-2-picrylhydrazyl
FTIR	Fourier transform infrared spectrum
HFIP	1,1,1,3,3,3,-hexafluoro-2-propanol
iNOS	inducible nitric oxide synthase
LDL	low density lipoprotein
PBS	phosphate buffered saline
P(LLA-CL)	poly(L-lactic acid-*co*-e-caprolactone)
S. aureus	*Staphylococcus aureus*
SEM	scanning electron microscopy
SF	silk fibroin
UV	ultraviolet
WAXD	wide-angle X-ray diffraction
XRD	X-ray diffraction

Acknowledgements This research was supported by the Independent Design Project of Key Scientific and Technological Innovation Team of

Zhejiang Province (Grant No. 2010R50012-19), the Key SRT Project of Jiaxing University (Grant No. 851713022), the National Natural Science Foundation of China (Grant No. 31271035), and Zhejiang Province Public Technology Applied Research Projects (Grant No. 2014C33005).

References

[1] Ammon H P, Wahl M A. Pharmacology of Curcuma longa. Planta Medica, 1991, 57(1): 1–7

[2] Gopinath D, Ahmed M R, Gomathi K, et al. Dermal wound healing processes with curcumin incorporated collagen films. Biomaterials, 2004, 25(10): 1911–1917

[3] Basnet P, Skalko-Basnet N. Curcumin: an anti-inflammatory molecule from a curry spice on the path to cancer treatment. Molecules, 2011, 16(6): 4567–4598

[4] Anand P, Kunnumakkara A B, Newman R A, et al. Bioavailability of curcumin: problems and promises. Molecular Pharmaceutics, 2007, 4(6): 807–818

[5] Kasoju N, Bora U. Fabrication and characterization of curcumin-releasing silk fibroin scaffold. Journal of Biomedical Materials Research Part B: Applied Biomaterials, 2012, 100(7): 1854–1866

[6] Pan C J, Shao Z Y, Tang J J, et al. *In vitro* studies of platelet adhesion, activation, and protein adsorption on curcumin-eluting biodegradable stent materials. Journal of Biomedical Materials Research Part A, 2007, 82(3): 740–746

[7] Brahatheeswaran D, Mathew A, Aswathy R G, et al. Hybrid fluorescent curcumin loaded zein electrospun nanofibrous scaffold for biomedical applications. Biomedical Materials, 2012, 7(4): 045001

[8] Gupta V, Aseh A, Ríos C N, et al. Fabrication and characterization of silk fibroin-derived curcumin nanoparticles for cancer therapy. International Journal of Nanomedicine, 2009, 4: 115–122

[9] Ali M M, Sarasa Bharati A A. Effect of crude extract of *Bombyx mori* coccoons in hyperlipidemia and atherosclerosis. Journal of Ayurveda and Integrative Medicine, 2011, 2(2): 72–78

[10] Murphy A R, St John P, Kaplan D L. Modification of silk fibroin using diazonium coupling chemistry and the effects on hMSC proliferation and differentiation. Biomaterials, 2008, 29(19): 2829–2838

[11] Zhang K, Wang H, Huang C, et al. Fabrication of silk fibroin blended P(LLA-CL) nanofibrous scaffolds for tissue engineering. Journal of Biomedical Materials Research Part A, 2010, 93(3): 984–993

[12] Zhang K H, Ye Q, Yan Z Y. Influence of post-treatment with 75% (v/v) ethanol vapor on the properties of SF/P(LLA-CL) nanofibrous scaffolds. International Journal of Molecular Sciences, 2012, 13(2): 2036–2047

[13] Zhang K H, Wu J L, Huang C, et al. Fabrication of silk fibroin/P(LLA-CL) aligned nanofibrous scaffolds for nerve tissue engineering. Macromolecular Materials and Engineering, 2013, 298 (5): 565–574

[14] Wang C Y, Zhang K H, Fan C Y, et al. Aligned natural-synthetic polyblend nanofibers for peripheral nerve regeneration. Acta Biomaterialia, 2011, 7(2): 634–643

[15] Blois M S. Antioxidant determinations by the use of a stable free radical. Nature, 1958, 181(4617): 1199–1200

[16] Kim K, Luu Y K, Chang C, et al. Incorporation and controlled release of a hydrophilic antibiotic using poly(lactide-*co*-glycolide)-based electrospun nanofibrous scaffolds. Journal of Controlled Release, 2004, 98(1): 47–56

[17] Suwantong O, Opanasopit P, Ruktanonchai U, et al. Electrospun cellulose acetate fiber mats containing curcumin and release characteristic of the herbal substance. Polymer, 2007, 48(26): 7546–7557

[18] Sun X Z, Williams G R, Hou X X, et al. Electrospun curcumin-loaded fibers with potential biomedical applications. Carbohydrate Polymers, 2013, 94(1): 147–153

[19] Chen X, Shao Z, Marinkovic N S, et al. Conformation transition kinetics of regenerated *Bombyx mori* silk fibroin membrane monitored by time-resolved FTIR spectroscopy. Biophysical Chemistry, 2001, 89(1): 25–34

[20] Tsuji H, Mizuno A, Ikada Y. Enhanced crystallization of poly-(L-lactide-*co*-ecaprolactone) during storage at room temperature. Journal of Applied Polymer Science, 2000, 76(6): 947–953

[21] Asakura T, Kuzuhara A, Tabeta R, et al. Conformational characterization of *Bombyx mori* silk fibroin in the solid state by high-frequency 13C cross polarization-magic angle spinning NMR, X-ray diffraction, and infrared spectroscopy. Macromolecules, 1985, 18(10): 1841–1845

[22] Zhang K H, Yin A L, Huang C, et al. Degradation of electrospun SF/P(LLA-CL) blended nanofibrous scaffolds *in vitro*. Polymer Degradation & Stability, 2011, 96(12): 2266–2275

[23] Hu M, Peng W, Li H J. Application of silk protein and its derivatives in cosmetics. Detergent and Cosmetics, 2011, 34: 34–39

[24] Sharma O P. Antioxidant activity of curcumin and related compounds. Biochemical Pharmacology, 1976, 25(15): 1811–1812